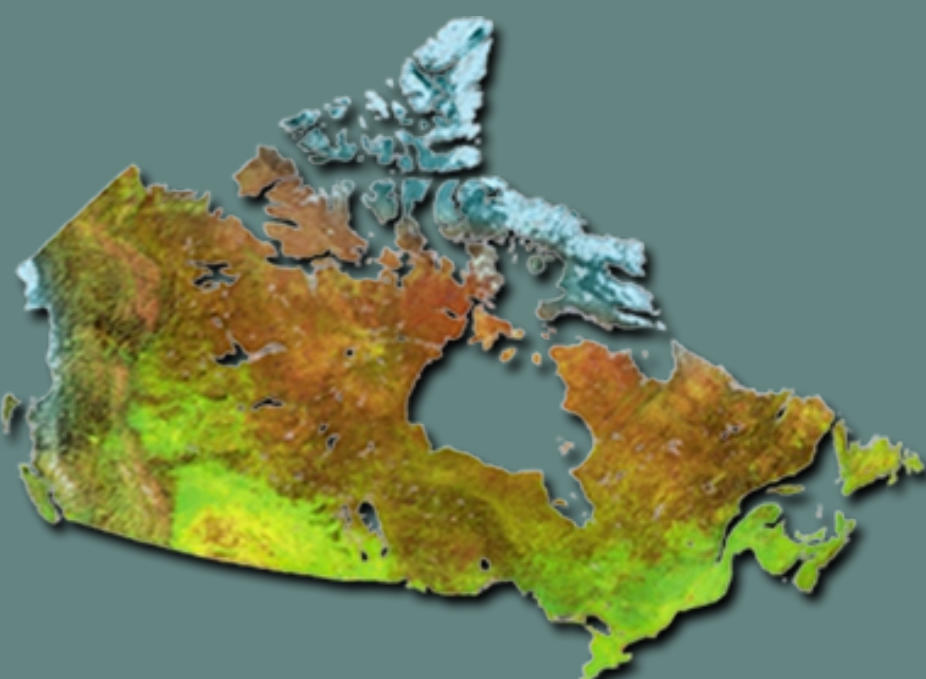# The Magmato-Hydrothermal Space: A New Metric for Geochemical Characterization of Ore Deposits

E.C. Grunsky[1], C.W. Brauhart[2], S. Hagemann[2], and B. Dubé[3]

http://www.cet.edu.au/research-projects/special-projects/projects/
osnaca-ore-samples-normalised-to-average-crustal-abundance

Introduction

It has long been recognized that different metal enrichments characterize different ore types (e.g., Lindgren, 1913). Modern geochemical techniques (e.g., Jackson and Sylvester, 2003) accurately quantify most ore and pathfinder element concentrations down to, or in many cases well below, average crustal abundance. There are thousands of descriptions in the published literature of ore deposit geochemistry covering the full gamut of hydrothermal and magmatic ores (e.g., Hedenquist et al., 2005). If metal associations are described with sufficient clarity, that information alone serves as a "fingerprint" or "signature" by which the style of mineralisation can be identified, or at least inferred.

Metal associations are recognized through quantitative assay data but normally described in a qualitative list format; e.g., Mortenson et al., (2010) describe Au-As-W-Cu-Pb-Zn enrichment for the Macraes gold deposit in New Zealand. Elements listed depend upon the assay suite, detection limits, and those elements the author judges to be significant enough to warrant inclusion. Only subjective means of comparison are available such as "very similar", "somewhat similar", "unrelated" or "completely different". For example a Zn-Pb-Ag-As-Tl-Sb enriched sample from a SHMS deposit has a *similar* signature to a Pb-Zn-Ag-Cd enriched sample of MVT mineralisation but *quite different* to a Zn-Cu-Ag-Au-Bi-Sn sample from a VHMS deposit and *very different* to a sample of massive Ni-Cu-Pt-Pd-Re mineralisation from a magmatic Ni-sulfide deposit. Furthermore, ore deposit geochemistry studies are normally restricted to a specific deposit, camp or class. A metric for comparison across the suite of major ore deposit classes has not been previously discussed in the literature with the exception of Drew et al. (1996).

The "Magmato-Hydrothermal Space" concept is presented as a new means to document and quantitatively describe both the range and statistical uniqueness of ore deposit types and clans. Magmato-Hydrothermal Space is a mathematical construct which, in this paper, uses 24 ore and pathfinder elements to discriminate different ore-signatures. However, the technique can be adapted for a greater or lesser number of variables as required. Two mathematical transforms are compared in terms of Magmato-Hydrothermal Space. First, OSNACA, which scales the data after log normalizing to average crustal abundance (Appendix 1). The OSNACA transform does not define an orthonormal space, which may create complications when statistical procedures are applied. Second, the log centered ratio (CLR) (Appendix 1) which does produce an orthonormal space (Aitchison, 1986), is applied to the same 24 elements. Thus, the CLR transform stands as a statistically more rigorous benchmark against which various statistical outputs from OSNACA transformed data can be compared.

Data

The amount of publicly available geochemical data for ore deposits is extensive, but analytical techniques, detection limits, and above all, assay suites, vary widely. The subset of samples that have been analyzed for all 24 ore and pathfinder elements used here, with appropriate detection limits, is extremely limited. In response to this gap in available data researchers at the Centre for Exploration Targeting at the University of Western Australia created the OSNACA database, a publicly available on-line resource providing consistent high-quality 63-element data for ore deposit samples from around the world (OSNACA, 2013).

Data presented here are for 431 "ore grade" samples from a current database of 519 samples (Fig.1). Iron and pegmatite ore samples have been excluded because they are not well discriminated by the 24 elements that define Magmato-Hydrothermal Space. Samples that do not contain at least one commodity above the following ppm cut-offs have also been excluded as "mineralized waste": Au(0.2), Pt(0.2), Pd(0.2), Ag(50), Cu(2000), Mo(500), Ni(2000), Pb(10000), Sn(2000), U(500), W(2000), Zn(10000).

Acknowledgements

Alex Christ and his team at Bureau Veritas – Ultratrace are warmly acknowledged for their tireless efforts in the laboratory and for their company's in-kind support. The OSNACA Project would not have been possible without generous funding from industry. CWB particularly acknowledges financial and logistical support from Sipa Resources Limited.

Results

Baysian Classification

The ore samples were grouped into ten classes based on sample description (provided by the donor). These classes are: Carlin Au, Epithermal, IOCG, MVT, Ni-Cu-PGE, Orogenic Au, Porphyry Cu, Sediment Hosted Cu, SHMS or VHMS and an eleventh grouped labelled "Other". The "other" samples were initially grouped into one of the ten primary classes, however later they were found to be gross statistical outliers and dropped from further evaluation. Linear Discriminant Analysis (LDA) was used to calculate posterior probabilities for 367 samples in the ten ore deposit classes. Both the CLR and OSNACA transformed data successfully classified more than 81% of samples, and many of the "misclassified" samples were transitional between two classes where overlap was expected; e.g., Orogenic Au – Epithermal, MVT – SHMS, and Porphyry Cu – IOCG (Tables 1 and 2).

MDS PCA and LDA Biplots

Multi Dimensional Scaling (MDS), Principal Component Analysis (PCA) and LDA are statistical techniques that aim to represent much of the variation in a multi-dimensional dataset in the first handful of components or axes. MDS provides the best visual discrimination for both the OSNACA (Fig. 2) and CLR transforms (Fig. 3). Linear relationships are significantly clearer for OSNACA transformed data in both MDS1-MDS2-MDS3 space (Figs 2a-b) and for individual elements versus one of the MDS axes (Figs 2c-e). MDS1 is positively correlated with Au and negatively correlated with Zn, whereas MDS2 is positively correlated with Cu and MDS3 is positively correlated with Ni.

Magmato-Hydrothermal Space

The ten ore deposit classes have been wireframed in MDS1-MDS2-MDS3 space for both the OSNACA transformed (Fig. 4) and CLR transformed data (not shown). Relationships between the ore deposit classes are similar for both, but significantly clearer for OSNACA transformed data. Other samples are presented as colored symbols with "Unknowns" as larger gray symbols.

Ore deposit wireframes overlap, despite there being very limited data for many of the ore deposit classes. The wireframes define a continuum from MVT and SHMS samples through VHMS, Sediment Hosted Cu, IOCG and Porphyry Copper to Orogenic Au and Carlin Au samples. Epithermal samples span the gap between Orogenic Au and VHMS samples and a group of IOCG samples protrude towards Ni-Cu-PGE samples.

Individual points include a cluster of Greisen and Porphyry Mo samples below the "Porphyry Cu" label (Fig. 4b), two green symbols to the right of the "Sed Cu" label representing the Phalabowra Carbonatite deposit (Fig. 4b) and larger grey symbols representing the Kanshansi and Sentinel copper deposits in front of the IOCG and Porphyry Cu wireframes (Fig. 4b).

Discussion

Numerous workers have suggested a continuum between different ore deposit classes such as MVT and SHMS (e.g., Leach et al., 2005), VHMS and Epithermal (e.g., Hannington et al., 1999), Orogenic Au, Carlin Au and Epithermal (Nesbitt, 1988) and even a link between IOCG deposits and mantle-related mineralisation (Groves et al., 2010). The overlapping relationships between wireframed sample populations (Fig. 4) shows that the transitions described by ore deposit researchers are mirrored in Magmato-Hydrothermal Space.

The continuum has two main "arms" (Fig. 4a). A "massive sulfide arm" extends from MVT samples through to Sediment-Hosted Cu samples and a "gold deposit arm" extends from Carlin and Epithermal samples through to Orogenic Au samples. The two arms meet at the IOCG and Porphyry Copper sample populations but are also linked by the Epithermal sample population that extends between VHMS and Orogenic Gold sample populations. In gross terms these arms represent the transition from low-temperature Zn-rich and Au-rich mineralisation respectively, to high temperature Cu-Au mineralisation where the two arms meet.

In the second view of Magmato-Hydrothermal Space (Fig. 4b), a vertical axis extends from "mantle related" Ni-rich mineralisation, through Cu-Au rich samples to granite associated mineralisation, whereas a horizontal axis represents the transition from sedimentary basin associated ores (Zn –rich) to igneous associated ores (Au-rich).

Conclusions

High-quality comprehensive whole-rock geochemical analyses of a wide range of ore deposit samples have allowed researchers on the OSNACA Project to define Magmato-Hydrothermal Space, a mathematical construct, in which a continuum of ore deposit signatures can be mapped. The broad architecture of Magmato-Hydrothermal Space reveals trends from low temperature Zn and Au mineralization that converge at high temperature Cu-Au mineralization, and a trend from mantle derived through to granite associated mineralization.

Further work is required to gather more data from the global inventory of ore deposit samples, research more detailed relationships within the data, and to better understand the statistical limitations inherent in the number space created by the OSNACA transform.
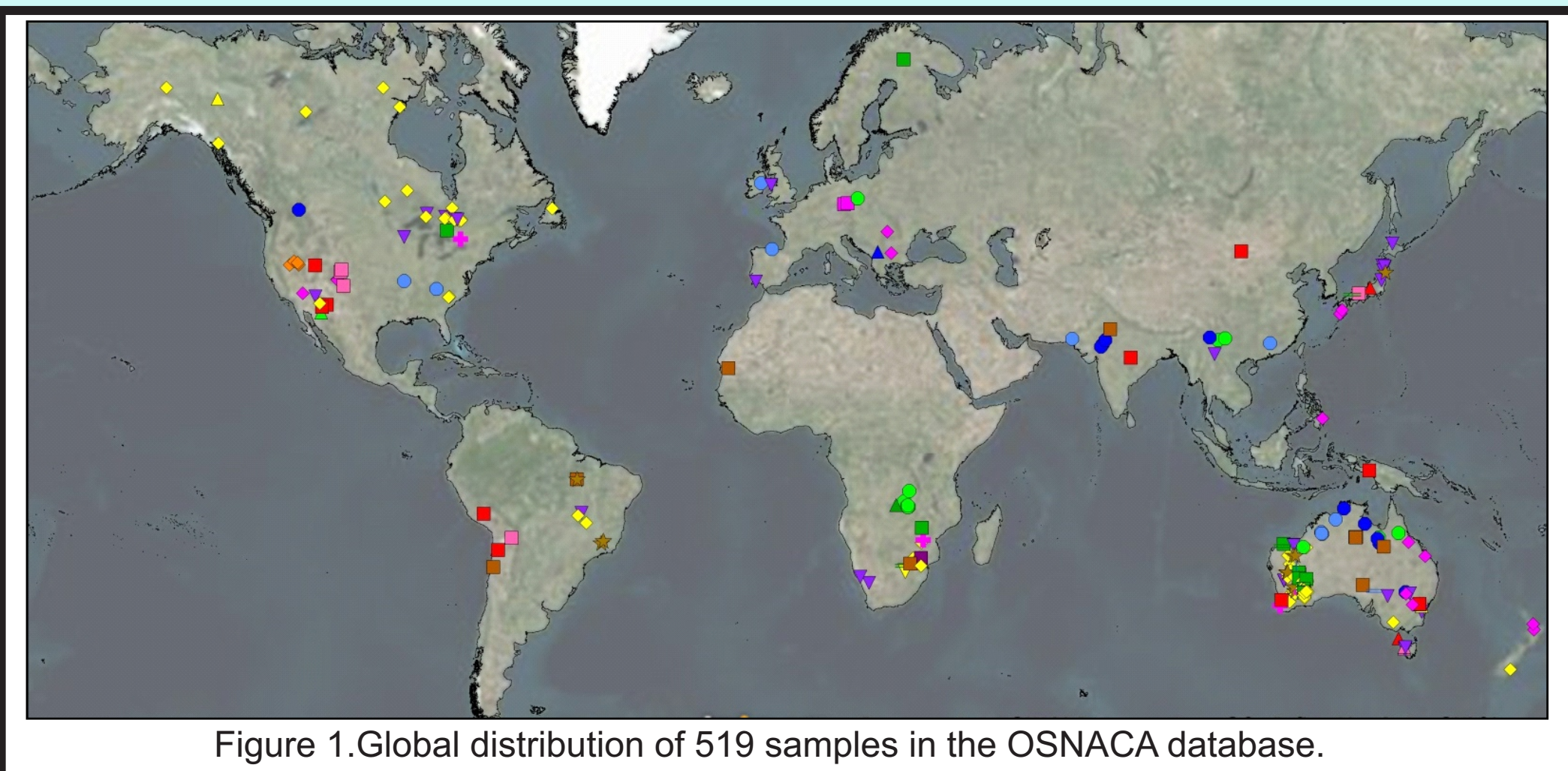

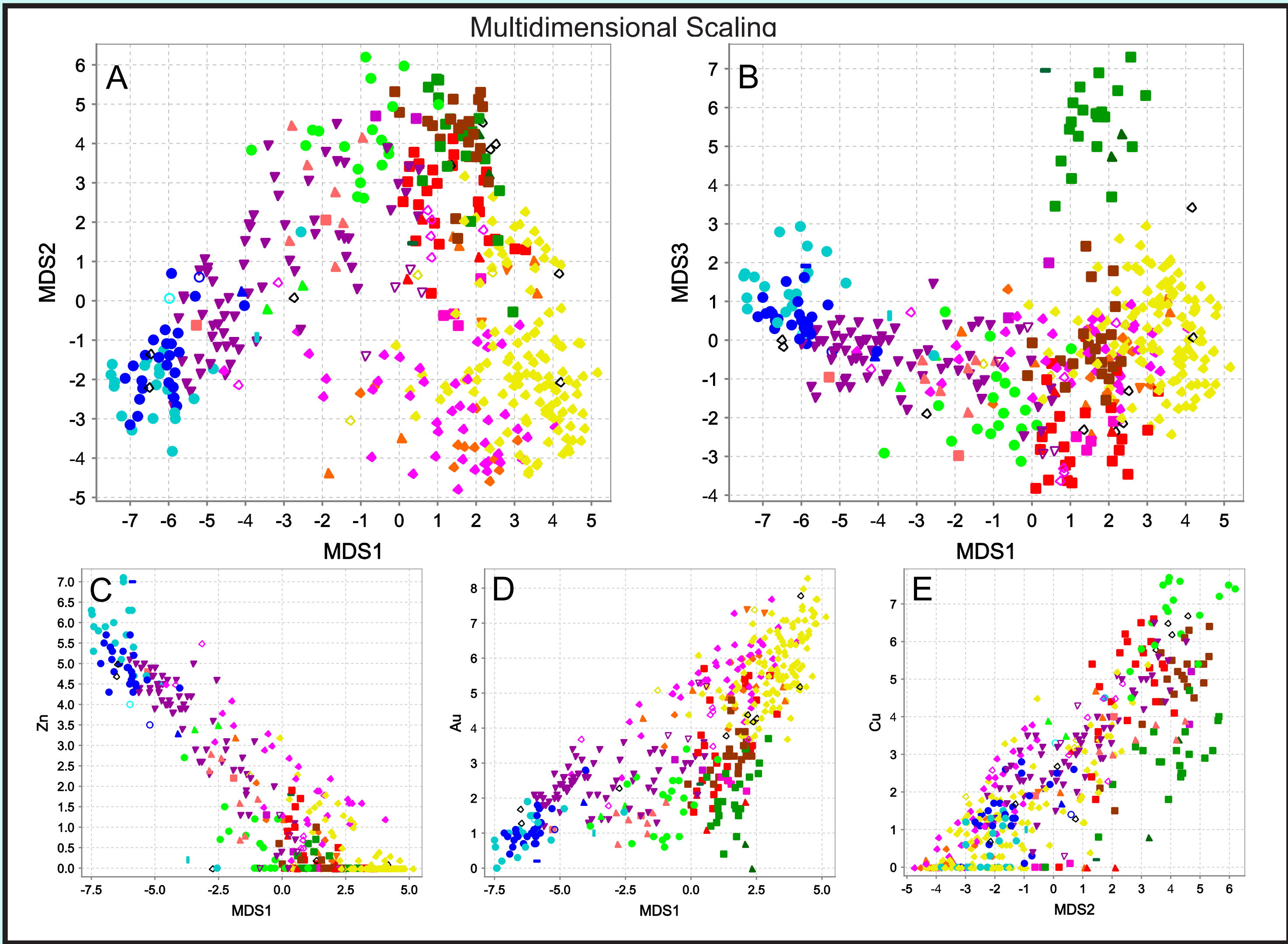Figure 1. Global distribution of 519 samples in the OSNACA database.

Figure 2. Bi-plots for OSNACA transformed data (legend as for Figure 1). A. MDS1 v MDS2, B. MDS1 v MDS3, C. MDS1 v Zn, D. MDS1 v Au, E. MDS2 v Cu.
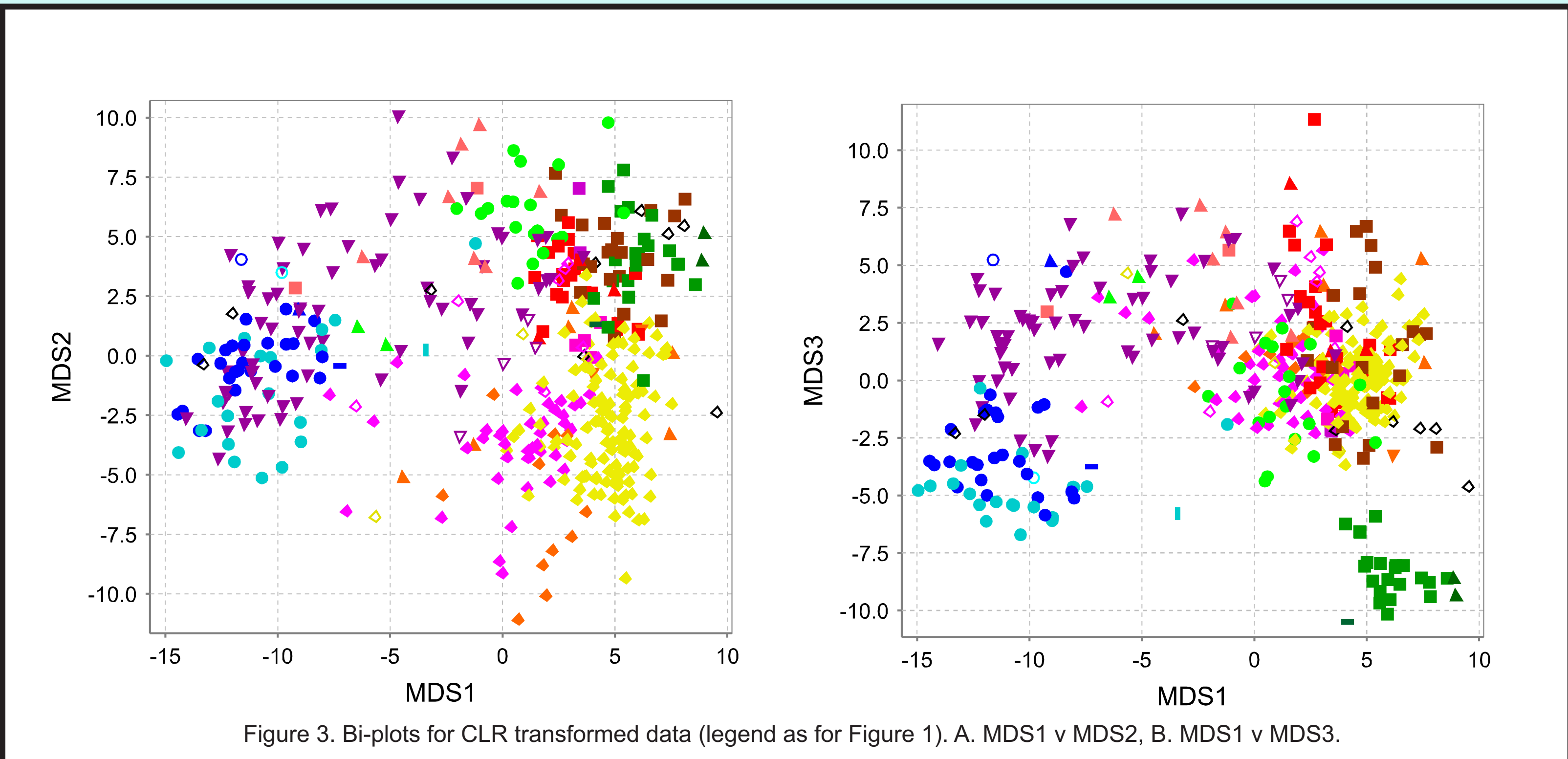

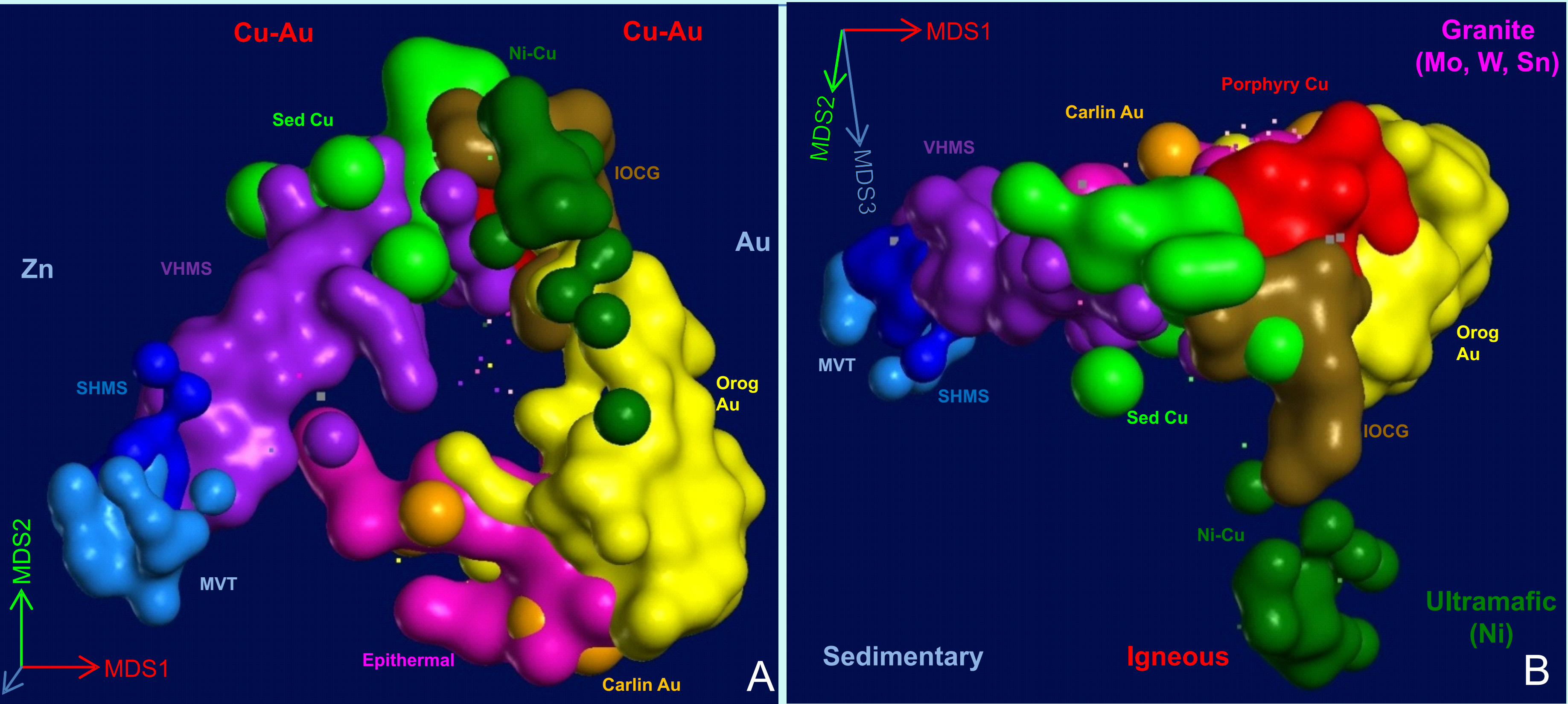Figure 3. Bi-plots for CLR transformed data (legend as for Figure 1). A. MDS1 v MDS2, B. MDS1 v MDS3.

Figure 4. Three dimensional views of "Magmato-Hydrothermal Space" defined by MDS1-MDS2-MDS3 for OSNACA transformed data showing wireframes of major sample populations and individual sample points of lesser populations.
A. View towards –MDS3.
B. Oblique view highlighting continuum from mantle to granite associated ore deposit samples and from sedimentary basin to igneous associated ore deposit samples.

Logcentred Transform

Centred Logratio (clr)
$$z_i = \log(x_i/g(x_D)) \quad (i = 1, \ldots, D),$$
where $g(x_D)$ is the geometric mean of the composition
Orthonormal but not full rank (Euclidean).

Appendix 1: OSNACA Transform

The OSNACA transform has four steps:
1. data below average crustal abundance (ACA) are replaced with ACA, or half the limit of detection, whichever is higher.
2. normalized to ACA
3. log transformed by $\log_{10}$ for elements with ACA <1 ppm, and $\log_6$ for elements with ACA > 1ppm, and
4. scaled to a fixed distance (10 units) from the origin.

Log, is applied such that a concentration of 100% returns a log score of 6. Average crustal abundance values are those of Rudnick and Gao (2003).

Data are censored to reduce the effect of lithological signals in the data. Censoring to ACA has a negligible effect on the definition of ore element signatures, given that ore-grade concentrations are typically at least two or three log units above ACA. Log normalization is applied with a variable log base to scale all ore and pathfinder elements to a comparable metric. Thus, log scores of zero represent average crustal abundance or lower, scores of one-two are anomalous to weakly mineralized, three are about ore grade, four-five are high to bonanza grade and six are ultra-high grade (or 100% concentration for more abundant elements).

References

Aitchison, J., 1986, The statistical analysis of compositional data. Monographs on statistics and applied probability. Chapman & Hall Ltd., London, 416 p.

Drew, L.J., and Menzie, D.W., 1993, Is there a metric for mineral deposit occurrence probabilities?: Nonrenewable Resources, v. 2. p. 92-105.

Groves, D.I., Bierlein, F.P., Meinert, L.D., and Hitzman M.W., 2010, Iron Oxide Copper-Gold (IOCG) deposits through Earth history: Implications for origin, lithospheric setting, and distinction from other epigenetic iron oxide deposits: Economic Geology, v. 105, p. 641-654.

Hannington, M.D., Poulsen, K.H., Thompson, J.F.H., and Sillitoe, R.H., 1999, Volcanogenic gold in the massive sulfide environment, *in* Barrie, C.T., and Hannington, M.D., eds., Volcanic-associated massive sulfide deposits: Processes and examples in modern and ancient settings: Reviews in Economic Geology 8, p. 325-356.

Hedenquist, J.W., Thompson, J.F.H., Goldfarb, R.J., and Richards J.R., editors, 2005, Economic Geology One Hundredth Anniversary Volume 1905 - 2005, 1136 p.

Jackson, S.E., and Sylvester, P.J., 2003, Applications of Laser-Ablation ICP-MS analysis: A tribute to Henry P. Longerich: The Canadian Mineralogist, v. 41, p. 257-258.

Leach, D.L., Sangster, D.F., Kelley, K.D., Large, R.R., Garven, G., Allen, C.R., Gutzmer, J. and Walters, S.G., 2005, Sediment-hosted lead-zinc deposits: A global perspective. Economic Geology, 100th Anniversary Volume: p. 561-607.

Lindgren, W., 1913. Mineral deposits. McGraw-Hill Book Company, New York, 883 p.

Mortensen, J.K., Craw, D., MacKenzie, D.J., Gabites, J.E., and Ullrich, T., 2010, Age and origin of orogenic gold mineralisation in the Otago Schist belt, South Island, New Zealand: Constraints from lead isotope and 40Ar/39Ar dating studies: Economic Geology, v. 105 p. 777-793.

Nesbitt, B.E., 1988, Gold deposit continuum: A genetic model for lode Au mineralization in the continental crust: Geology, v. 16, p. 1044-1048.

OSNACA, 2013, OSNACA: Ore samples normalized to average crustal abundance: http://www.cet.edu.au/research-projects/special-projects/projects/osnaca-ore-samples-normalised-to-average-crustal-abundance (December 2013).

Rudnick, R.L., and Gao, S., 2003, The composition of the continental crust, *in* Rudnick R.L., ed., The crust, Vol. 3, Holland H.D., and Turekian K.K., eds., Treatise on Geochemistry, Elsevier-Pergamon, Oxford, p. 1-64.

TABLE 1. POSTERIOR-PROBABILITY MATRIX AFTER LINEAR DISCRIMINANT ANALYSIS OF CLR-TRANSFORMED DATA

	Carlin	Epithermal	IOCG	MVT	Nickel	Orogenic Au	Porphyry Cu	SHMS	Sed Cu	VHMS
Carlin	8	1	0	0	0	2	0	0	0	0
Epithermal	4	23	0	0	0	14	0	1	0	1
IOCG	0	0	15	0	0	0	5	0	1	0
MVT	0	0	0	14	0	0	0	5	1	0
Nickel	0	0	0	0	21	0	0	0	0	0
Orogenic Au	0	1	1	0	0	117	2	0	0	0
Porphyry Cu	0	0	3	0	0	2	14	0	0	0
SHMS	0	0	0	3	0	0	0	18	0	4
Sed. Cu	0	0	0	0	0	0	0	0	18	1
VHMS	0	1	2	0	0	0	5	6	1	52

TABLE 2. POSTERIOR-PROBABILITY MATRIX AFTER LINEAR DISCRIMINANT ANALYSIS OF OSNACA-TRANSFORMED DATA

	Carlin	Epithermal	IOCG	MVT	Nickel	Orogenic Au	Porphyry Cu	SHMS	Sed Cu	VHMS
Carlin	10	0	0	0	0	0	0	0	0	1
Epithermal	3	27	0	0	0	11	0	1	0	1
IOCG	0	0	19	0	0	1	1	0	0	0
MVT	0	0	0	13	0	0	0	6	1	0
Nickel	0	0	0	0	21	0	0	0	0	0
Orogenic Au	2	4	2	0	0	108	5	0	0	0
Porphyry Cu	0	0	3	0	0	2	14	0	0	0
SHMS	0	0	0	3	0	0	0	19	0	3
Sed. Cu	0	0	0	0	0	0	0	0	18	1
VHMS	0	0	2	0	0	0	5	9	1	50